Temporally precise *in vivo* control of intracellular signalling

Raag D. Airan[1], Kimberly R. Thompson[1], Lief E. Fenno[1], Hannah Bernstein[1] & Karl Deisseroth[1,2]

In the study of complex mammalian behaviours, technological limitations have prevented spatiotemporally precise control over intracellular signalling processes. Here we report the development of a versatile family of genetically encoded optical tools ('optoXRs') that leverage common structure–function relationships[1] among G-protein-coupled receptors (GPCRs) to recruit and control, with high spatiotemporal precision, receptor-initiated biochemical signalling pathways. In particular, we have developed and characterized two optoXRs that selectively recruit distinct, targeted signalling pathways in response to light. The two optoXRs exerted opposing effects on spike firing in nucleus accumbens *in vivo*, and precisely timed optoXR photostimulation in nucleus accumbens by itself sufficed to drive conditioned place preference in freely moving mice. The optoXR approach allows testing of hypotheses regarding the causal impact of biochemical signalling in behaving mammals, in a targetable and temporally precise manner.

To enable optical control over intracellular signalling in mammals (Fig. 1a), we capitalized on shared structure–function relationships[1] among GPCRs to develop and express *in vivo* multiple distinct opsin/GPCR[2] chimaeras with novel transduction logic that couples signal to effector. In principle, a chimaeric opsin-receptor protein engineered to be functional within mammals *in vivo*, targetable to specific cells, and responsive to precisely timed light pulses would be of substantial interest for physiology. Such an approach could take advantage of the speed of optics to test the importance of (1) intracellular biochemical events at precisely defined behaviourally relevant times, (2) pulsatile versus tonic modulation, (3) synchrony between different modulatory systems, and many other fundamental physiological and pathological processes in defined cell types over a range of timescales. Whereas much is known about GPCR structure–function relationships from mutants and chimaeras[1–3], *in vivo* application of this knowledge for optical interventional purposes had not been considered feasible as it is not generally practical to supply chemical cofactors (in this case retinoids, to allow opsin function by transduction of the light signal) to intact mammalian tissues and circuits *in vivo*. However, recent work on microbial opsins has revealed that the mammalian brain[4] contains sufficient retinoid levels to allow opsin function without addition of cofactors. Here we capitalize on this knowledge to develop opsin-receptor chimaeras (the optoXR family) as a new class of *in vivo* physiology tools.
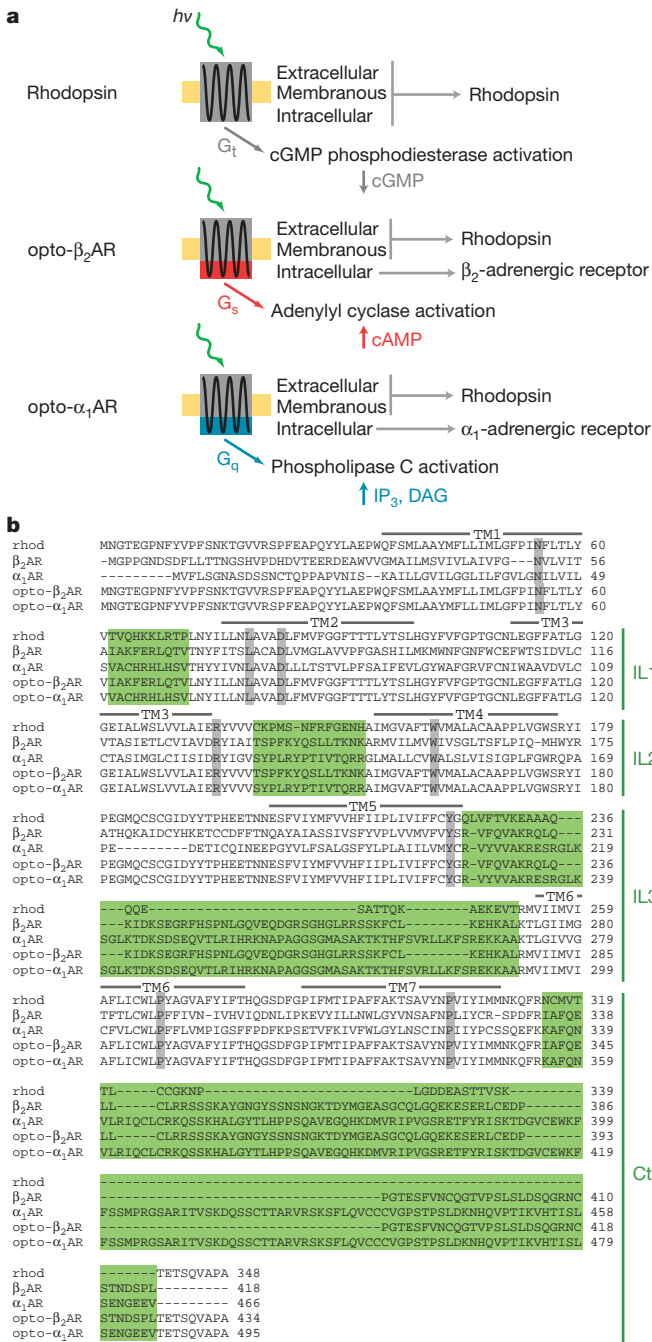
To validate this concept in mammals, the intracellular loops of rhodopsin were replaced with those of specific adrenergic receptors by first aligning conserved[5] residues of the G_q-coupled human α_{1a}-adrenergic receptor (α_1AR; NCBI accession no. NP_000671) and the G_s-coupled hamster β_2-adrenergic receptor (β_2AR; NCBI accession no. CAA27430) with the G_t-coupled bovine rhodopsin (NCBI accession no. P02699; Fig. 1a,b). We then engineered exchanges of intracellular regions (including carboxy-terminal domains, as in ref. 2) for

each receptor based on structural models[2,6] (Fig. 1b) to transfer G-protein coupling from G_t, and optimized each receptor for *in vivo* expression in mammals. Upon activation by varied ligands, the native receptors can explore multiple ensemble states to recruit canonical and non-canonical pathways in the recently described phenomenon of ligand-biased signalling[7–9]. The optoXRs are likely to select a single active ensemble state upon sensing light in a manner dependent on biological context[7–9].

We constructed genes encoding chimaeras (opto-α_1AR and opto-β_2AR) fused to a fluorescent protein. To validate functional optoXR expression, we imaged $[Ca^{2+}]_i$ (intracellular calcium concentration) in HEK cells transfected with opto-α_1AR alone (expected to recruit $[Ca^{2+}]_i$ via G_q), or with both opto-β_2AR (expected to recruit cyclic AMP via G_s) and the cAMP-gated Ca^{2+} channel CNGA2-C460W/E583M[10]. Ratiometric $[Ca^{2+}]_i$ imaging demonstrated that 60 s of green light stimulation (504 ± 6 nm, 7 mW mm^{-2}) was sufficient to drive prominent $[Ca^{2+}]_i$ signals downstream of either optoXR but not in control conditions (Fig. 1c), revealing functional expression. To test specificity of the signalling controlled by each optoXR, transduced HEK cells were illuminated with 3 mW mm^{-2} 504 ± 6 nm light for 60 s and then lysed and analysed for levels of cGMP, cAMP and IP$_1$ (a degradation product of IP$_3$) via immunoassays (Methods). We observed the canonical pattern expected for opto-β_2AR corresponding to its molecular design, as optical stimulation yielded significant production of cAMP in opto-β_2AR-expressing cells (Fig. 2a, top), comparable to that achieved with pharmacological stimulation of the wild-type β_2AR and without recruitment of IP$_3$ (Fig. 2a, middle), $[Ca^{2+}]_i$ (Fig. 1c), or substantial dark activity. In contrast, optical stimulation yielded significant upregulation of IP$_3$ signalling in opto-α_1AR-expressing cells (Fig. 2a, middle), comparable to levels induced by pharmacological stimulation of the wild-type α_1AR. Together with the $[Ca^{2+}]_i$ elevations (Fig. 1c), these data reveal the pattern expected for G_q recruitment, a pattern not seen in opto-β_2AR-expressing cells (Fig. 2a, top). Optical stimulation of cells expressing either construct was unable to modulate cGMP levels (Fig. 2a, bottom), further indicating the signalling specificity of the chimaeric proteins. Similar assays revealed that the optoXRs retain an action spectrum close to that of native rhodopsin, are able to integrate signals over a range of biologically suitable light fluxes (Supplementary Fig. 1a), and can activate non-canonical pathways to a similar extent as wild-type receptors, as shown for p42/p44-MAPK signalling (Supplementary Fig. 1b, top).

We next tested optoXR performance in intact neural tissue, to determine if supplementation of retinal cofactors would be required. Lentiviral vectors carrying the optoXR fusion genes under control of the synapsin-I promoter (to target biochemical modulation to local neurons rather than other potentially G_s/G_q-responsive cellular tissue elements such as glia and endothelial cells; Fig. 2b, top left) were stereotactically injected into the nucleus accumbens of adult mice

[1]Department of Bioengineering, [2]Department of Psychiatry & Behavioral Sciences, Stanford University, Stanford, California 94305, USA.

a

b

```
                   TM1
rhod        MNGTEGPNFYVPFSNKTGVVRSPFEAPQYYLAEPWQFSMLAAYMFLLIMLGFPINFLTLY  60
β₂AR        -MGPPGNDSDFLLTTNGSHVPDHDVTEERDEAWVVGMAILMSVIVLAIVFG---NVLVIT  56
α₁AR        --MVFLSGNASDSSNCTQPPAPVNIS--KAILLGVILGGLILFGVLGNILVIL          49
opto-β₂AR   MNGTEGPNFYVPFSNKTGVVRSPFEAPQYYLAEPWQFSMLAAYMFLLIMLGFPINFLTLY  60
opto-α₁AR   MNGTEGPNFYVPFSNKTGVVRSPFEAPQYYLAEPWQFSMLAAYMFLLIMLGFPINFLTLY  60

               TM2                              TM3
rhod        VTVQHKKLRTPLNYILLNLAVADLFMVFGGFTTTLYTSLHGYFVFGPTGCNLEGFFATLG  120      IL1
β₂AR        AIAKFERLQTVLNYITSLACADLVMGLAVVPFGASHILMKMWNFGNFWCEFWTSIDVLC   116
α₁AR        SVACHRHLHSVTHYYIVNLAVADLLLTSTVLPFSAIFEVLGYWAFGRVFCNIWAAVDVLC  109
opto-β₂AR   VIAKFERLQTVLNYILLNLAVADLFMVFGGFTTTLYTSLHGYFVFGPTGCNLEGFFATLG  120
opto-α₁AR   GEIALWSLVVLAIERYVVVCKPMS-NFRFGENHAIMGVAFTWVMALACAAPLVGWSRYI   180

               TM3                              TM4
rhod        GEIALWSLVVLAIERYVVVCKPMS-NFRFGENHAIMGVAFTWVMALACAAPLVGWSRYI   179      IL2
β₂AR        VTASIETLCVIAVDRYIAITSPFKYQSLLTKNKARMVILMVWIVSGLTSFLPIQ-MHWYR  175
α₁AR        CTASIMGLCIISIDRYIGVSYPLRYPTIVTQRRGLMALLCVWALSLVISIGPLFGWRQPA  169
opto-β₂AR   GEIALWSLVVLAIERYVVVTSPFKYQSLLTKNKARMVILMVWIVSGLTSFLPIQ-MHWYR  180
opto-α₁AR   GEIALWSLVVLAIERYVVVSYPLRYPTIVTQRRAIMGVAFTWVMALACAAPLVGWSRYI   180

               TM5
rhod        PEGMQCSCGIDYYTPHEETNNESFVIYMFVVHFIIPLIVIFFCYGQLVFTVKEAAAQ---  236      IL3
β₂AR        ATHQKAIDCYHKETCCDFFTNQAYAIASSIVSFYVPLVVMVFVYSR-VFQVAKRQLQ--- 231
α₁AR        PE--------DETICQINEEPGYVLFSALGSFYLPLAIILVMYCR-VYVVAKRESRGLK   219
opto-β₂AR   PEGMQCSCGIDYYTPHEETNNESFVIYMFVVHFIIPLIVIFFCYGR-VFQVAKRQLQ--- 236
opto-α₁AR   PEGMQCSCGIDYYTPHEETNNESFVIYMFVVHFIIPLIVIFFCYGR-VYVVAKRESRGLK  239

rhod        ---QQE------------------------SATTQK---------AEKEVTRMVIIMVI   259
β₂AR        ---KIDKSEGRFHSPNLGQVEQDGRSGHGLRRSSKFCL-------KEHKALKTLGIIMG   280
α₁AR        SGLKTDKSDSEQVTLRIHRKNAPAGGSGMASAKTKTHFSVRLLKFSREKKAAKTLGIVVG  279
opto-β₂AR   ---KIDKSEGRFHSPNLGQVEQDGRSGHGLRRSSKFCL-------KEHKALRMVIIMVI   285
opto-α₁AR   SGLKTDKSDSEQVTLRIHRKNAPAGGSGMASAKTKTHFSVRLLKFSREKKAARMVIIMVI  299

               TM6                              TM7
rhod        AFLICWLPYAGVAFYIFTHQGSDFGPIFMTIPAFFAKTSAVYNPVIYIMMNKQFRNCMVT  319
β₂AR        TFTLCWLPFFIVN-IVHVIQDNLIPKEVYILLNWLGYVNSAFNPLIYCR-SPDFRIAFQE  338
α₁AR        CFVLCWLPFFLVMPIGSFFPDFKPSETVFKIVFWLGYLNSCINPIIYPCSSQEFKKAFQN  339
opto-β₂AR   AFLICWLPYAGVAFYIFTHQGSDFGPIFMTIPAFFAKTSAVYNPVIYCR-IAFQE      345
opto-α₁AR   AFLICWLPYAGVAFYIFTHQGSDFGPIFMTIPAFFAKTSAVYNPVIYIMMNKQFRKAFQN  359

rhod        TL-----CCGKNP-----------------------LGDDEASTTVSK----------   339
β₂AR        LL-----CLRRSSSKAYGNGYSSNSNGKTDYMGEASGCQLGQEKESERLCEDP------  386
α₁AR        VLRIQCLCRKQSSKHALGYTLHPPSQAVEGQHKDMVRIPVGSRETFYRISKTDGVCEWKF  399
opto-β₂AR   LL-----CLRRSSSKAYGNGYSSNSNGKTDYMGEASGCQLGQEKESERLCEDP------  393      Ct
opto-α₁AR   VLRIQCLCRKQSSKHALGYTLHPPSQAVEGQHKDMVRIPVGSRETFYRISKTDGVCEWKF  419

rhod        --------------------------------PGTESFVNCQGTVPSLSLDSQGRNC   410
β₂AR        FSSMPRGSARITVSKDQSSCTTARVRSKSFLQVCCCVGPSTPSLDKNHQVPTIKVHTISL  458
α₁AR        PGTESFVNCQGTVPSLSLDSQGRNC   418
opto-β₂AR   --------------------------------PGTESFVNCQGTVPSLSLDSQGRNC   418
opto-α₁AR   FSSMPRGSARITVSKDQSSCTTARVRSKSFLQVCCCVGPSTPSLDKNHQVPTIKVHTISL  479

rhod        -------TETSQVAPA   348
β₂AR        STNDSPL--------   418
α₁AR        SENGEEV--------   466
opto-β₂AR   STNDSPLTETSQVAPA   434
opto-α₁AR   SENGEEVTETSQVAPA   495
```

c

Figure 1 | OptoXR: optogenetic control of intracellular signal transduction. **a**, OptoXR design; DAG, diacylglycerol. **b**, Primary structure alignment of wild-type GPCRs (Rhodopsin (rhod), β_2AR, α_1AR) and optoXRs (opto-β_2AR, opto-α_1AR); grey, highly conserved residues; green, swapped intracellular domains (IL, intracellular loop; Ct, C terminus; TM, transmembrane domains). **c**, Fura-2 Ca^{2+} imaging. Mean ± s.e.m. (shading) traces of HEK cells transfected with opto-α_1AR alone (red; 92 cells over 3 coverslips); opto-β_2AR cotransfected with cAMP-gated calcium channel (CNGA2-C460W/E583M; blue; 120 cells over 3 coverslips); opto-β_2AR alone (light grey; 26 cells over 2 coverslips); mCherry cotransfected with CNGA2 (dark grey; 40 cells over 2 coverslips) during 60 s of 500 nm light (green bar; 7 mW mm^{-2}) following 30 s baseline. (Two-tailed Student's t-test of signals at end of light stimulation versus baseline; n.s., $P > 0.05$; ***$P < 0.001$.) Inset, pseudocolour images of fura-2 ratio before (left; 'no stim.' at 0 s) and after (right; 'stim.' at 150 s) stimulation. dR, fractional change in 340/380 fluorescence excitation ratio. Scale bar, 100 μm.

(Methods). In contrast to pharmacological or electrical interventions, this strategy targets biochemical modulation to neurons with somatodendritic compartments in accumbens (~95% GABAergic medium spiny neurons[11], without further subtype specificity; Fig. 2b, left) and excludes fibres of passage or afferent presynaptic terminals as these lentiviruses do not transduce cells via axons[12]. Two weeks after transduction, acute coronal slices of accumbens were prepared in artificial cerebrospinal fluid, optically stimulated for 10 min, and immediately fixed and stained for Ser 133-phosphorylated CREB (pCREB), a biochemical integrator of both cAMP and Ca^{2+}-coupled signalling cascades[13]. Indeed, without supplementation of exogenous retinoids, we observed significantly elevated pCREB in the optoXR-expressing populations (Fig. 2b, right, Supplementary Table 1) and not in non-illuminated tissue (Supplementary Fig. 1b, bottom).

We also determined the functional consequences of optoXR activation on accumbens local electrical activity by recording multiunit *in vivo* neuronal firing with an optrode[12] targeted to transduced accumbens (Fig. 3a). No significant differences in baseline firing rates were observed in the dark with either construct (Fig. 3a, bottom right; Supplementary Table 2; Supplementary Fig. 2a). Interestingly, optical stimulation resulted in decreased network firing in opto-β_2AR-expressing accumbens (left trace in Fig. 3b illustrates effect kinetics; summary data shown in Fig. 3c and d respectively; raw data and description of calculations in Supplementary Table 3 and Supplementary Fig. 2b), in agreement with previous pharmacological studies targeting G_s (ref. 14). In contrast, optical stimulation increased firing in opto-α_1AR-expressing accumbens (Fig. 3b right; Fig. 3c, d). Spike frequency histograms showed that the kinetics of optoXR effects on firing rates was consistent with biochemical rather than electrical initiation of the signal (Fig. 3d, Supplementary Fig. 2). These electrophysiological data, in combination with the earlier biochemical validations, support the conclusion that optoXRs can be functionally expressed *in vivo*, to permit differential photoactivatable control of intracellular cascades and to modulate network physiology.

We next took an optogenetic approach to assess the ability of precisely timed optoXR stimulation to modulate behaviour[15] in freely moving mice. Portable solid-state light delivery was combined with transgenic expression of optoXRs to optically control intracellular signalling within accumbens neurons in the temporally precise manner required for operant behaviour (Fig. 4a)[4,12]. Confocal analysis revealed expression to be limited to local accumbens neurons; in particular no labelling was observed in afferent fibres, in distant regions projecting to accumbens, in glia, or in surrounding regions (Supplementary Fig. 3). We targeted optical stimulation to transduced accumbens as part of a three-day operant conditioned place preference assay (Fig. 4a, Supplementary Fig. 3; Methods). On each day of the experimental test, animals were allowed to freely explore the place preference apparatus (Fig. 4a, bottom). On day 1, animals freely explored the apparatus without optical stimulation. On day 2, whenever the animal freely entered the designated conditioned chamber, a laser-diode-coupled optical fibre registered to the transduced region delivered light pulses at 10 Hz to approximate the likely intensity of monoaminergic input
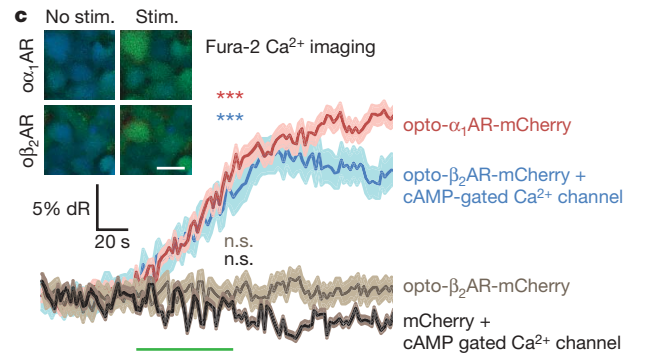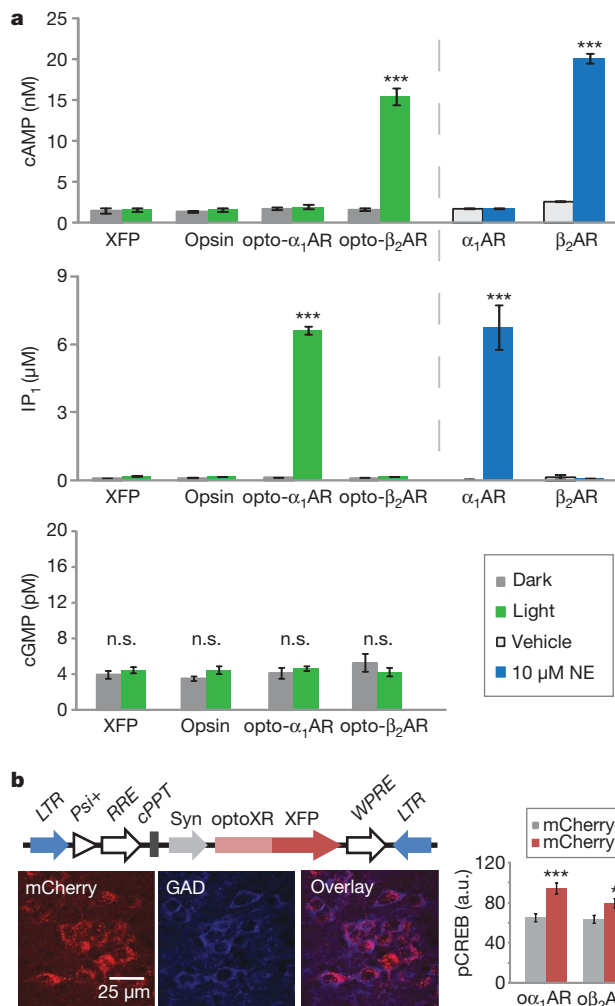
Figure 2 | Signalling specificity and *in vivo* functionality. a, HEK cells expressing indicated construct, stimulated with light for 60 s (left) or 10 μM norepinephrine for 5 min (NE; right), and immunoassayed for indicated intracellular messenger. Opsin, rhodopsin; XFP, fluorescent protein (YFP) alone; IP_1, degradation product of IP_3 (Student's *t*-test; $n = 3$ wells per condition; n.s., $P > 0.05$, ***$P < 0.001$). **b**, Top left, lentiviral expression vector of optoXRs under neuron-specific synapsin-I promoter (Syn). LTR, RRE, elements necessary for viral replication; Psi+, element necessary for viral packaging; WPRE, cPPT, elements for stable expression. Bottom left, GAD immunostaining of opto-α_1AR-expressing cells. No expression seen in glia, fibres of passage, or neurons outside or projecting to accumbens. Right, significant pCREB activation observed in optoXR-expressing cells (mCherry+) following 10 min optical stimulation of acute accumbens slices ($n = 38$–51 cells pooled from 3 slices per group; ANOVA, Tukey's post-hoc tests, $F_{3,173} = 9.853$, *$P < 0.05$, ***$P < 0.001$; numerical data in Supplementary Table 1). oα_1AR, opto-α1AR; oβ_2AR, opto-β_2AR; a.u., arbitrary units.

during strong reward[16,17]. Path tracing revealed that the flexible optical-fibre approach allowed full and unimpeded exploration of all chambers (Fig. 4a, bottom). On day 3, animals again freely explored the apparatus without optical stimulation, and the time spent in the conditioned chamber was quantified by two independent, blinded scorers. Notably, animals expressing opto-α_1AR showed a robust increase in preference for the conditioned side of the apparatus following optical stimulation (Fig. 4b, Supplementary Table 4). This effect of temporally precise biochemical modulation was reproducible across two separate cohorts of opto-α_1AR animals ($n = 5$–6, $P < 0.05$, Student's *t*-test for each cohort for time in conditioned chamber; $n = 11$, $P < 0.01$ for the total population), whereas the other opsin genes, opto-β_2AR and ChR2, appeared less effective in driving preference (Fig. 4, Supplementary Fig. 4; Supplementary Table 4).
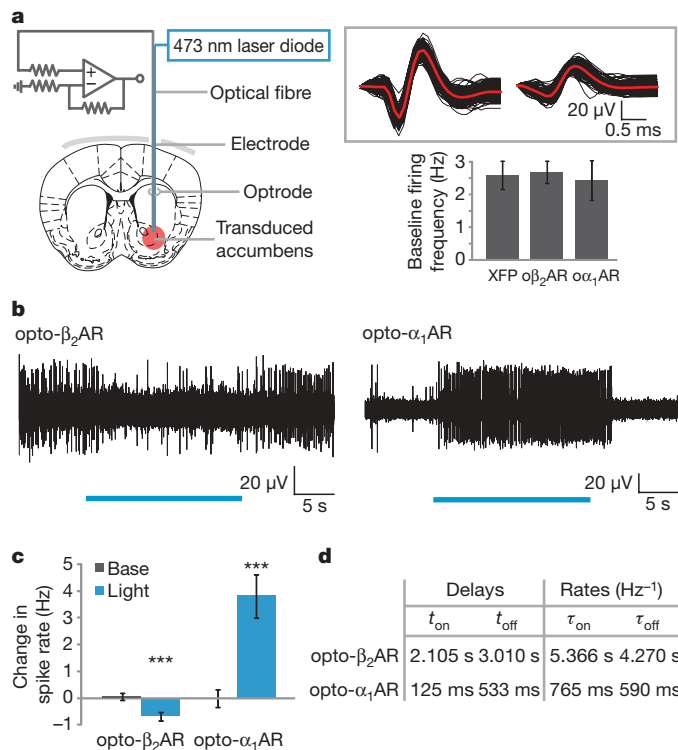
Figure 3 | *In vivo* optoXR modulation of neural activity. a, Optrode targeted to transduced accumbens for multiunit recordings. Top right, spike waveforms from single trace; red, average waveform. Bottom right, baseline firing rates for indicated construct; XFP, transduced with fluorescent protein (mCherry) alone. ($n = 54$ traces, XFP; 30 traces, opto-β_2AR; 18 traces, opto-α_1AR. Mean ± s.e.m.: XFP, 2.59 ± 0.44 Hz; opto-α_1AR, 2.44 ± 0.60 Hz; opto-β_2AR, 2.69 ± 0.35 Hz; numerical data in Supplementary Table 2 and Supplementary Fig. 2.) **b**, *In vivo* optrode recordings of opto-β_2AR (left) and opto-α_1AR (right) with light stimulation (blue bar). **c**, Change in spiking frequency with light versus baseline (opto-β_2AR: $n = 30$ traces from 2 animals, 5–7 traces per recording site; and opto-α_1AR: $n = 18$ traces from 2 animals, 4–5 traces per recording site, two-tailed Student's *t*-test, ***$P < 0.001$; numerical data in Supplementary Table 3). **d**, Firing rate change kinetics; see Supplementary Fig. 2.

The effect of opto-α_1AR stimulation in accumbens neurons was specific to reward-related behaviour and did not extend to direct modulation of anxiety-related behaviours or locomotor activity, as identical optical stimulation delivered to a cohort of the same animals in an open field test (Methods) revealed no significant effect on distance travelled or preference for wall proximity (Fig. 4c; Supplementary Fig. 4c).

Previously, microbial opsin optogenetics has been developed and applied to achieve fast, cell-type-targeted optical control of membrane voltage in neurons. Beyond membrane voltage, biochemical modulation of cell populations may also contribute to the internal representations of behaviourally relevant brain states, both in excitable and in non-excitable cells. The results presented here demonstrate optogenetic control of intracellular signalling that is temporally precise, operates *in vivo* within behaving mammals, displays extremely low dark activity, and recruits the complex fabric of multiple signalling molecules downstream of native receptors, thereby unifying in a single technology many of the individual positive aspects of other approaches[18–24]. A similar approach could be used to probe directly the causal significance of seven-transmembrane-dependent signalling pathways triggered by other modulators, including myriad neurotransmitters and endocrine hormones[3]. Indeed, the optoXR approach could be extended beyond excitable cells to probe causal significance of temporally precise biochemical signalling in diverse non-excitable tissues, capitalizing upon the versatile integration of fibre-optic depth targeting with optogenetically targeted photosensitivity.
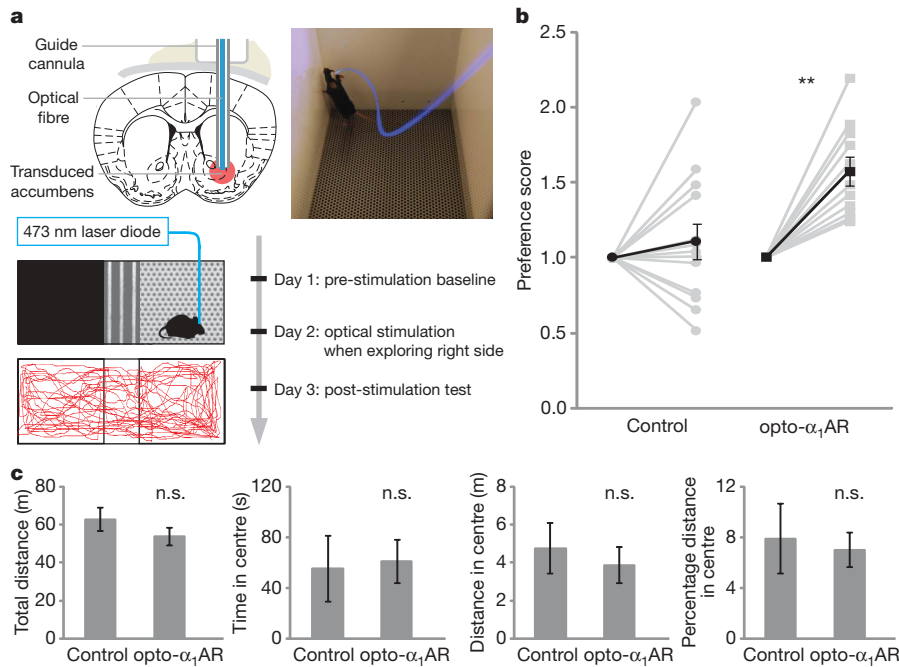
Figure 4 | Optical control of reward-related behaviour. a, Top left, stereotactic targeting of transduced region *in vivo*. Top right, freely moving mouse with implanted fibre optic. Bottom, schematic of place preference apparatus and test; trace of mouse freely exploring apparatus. **b,** Individual (grey) and mean (black) preference (fold increased time in conditioned chamber) (Control: injected with vehicle alone; $n = 11$, 13 animals per group; two-tailed Student's *t*-test, **$P < 0.01$; mean ± s.e.m.; numerical data in Supplementary Table 4). **c,** 15 min open field test with 10 Hz light stimulation. ($n = 3$, 4 animals per group, two-tailed Student's *t*-test, n.s., not significant).

As noted above, it will be important to carefully consider the phenomenon of ligand-biased signalling[8,9], wherein varied ligands can stabilize ensemble receptor conformational states and thereby bias the intracellular action of the receptor in coupling to alternative transduction cascades. The optoXRs can indeed induce these alternative cascades to similar levels as with pharmacological manipulation (for example, opto-β_2AR can induce similar changes in MAPK activation compared with native ligand acting on the wild-type β_2AR; Supplementary Fig. 1b, top); however, individual optoXRs may not always be found to permit control of all of the conformational states that contribute to ligand-biased signalling. Retinal-based tools do provide unique advantages, including the presence of the endogenous chromophore in mammalian tissues, and the fact that these retinal-based tools display extremely low activity in the dark[3,25]. Optogenetics therefore can take the form of diverse effectors linked to fast, single-component retinal-binding modules, capitalizing on the temporal precision of optics.

In summary, the optoXR method complements microbial opsin strategies, providing another dimension of fast, targetable cellular control operative in behaving mammals. In the future, wavelength-shifted versions of the optoXRs, based on known opsin genes with different action spectra, may provide still further possibilities for separable channels of biochemical and electrical control. Together, these technologies could be integrated with fast circuit readout technologies for increasingly sophisticated interrogation and reverse-engineering of neural circuitry, both in normal operation and in disease states[26–30].

METHODS SUMMARY

***In vivo* recording and analysis.** Optrodes consisting of a multi-mode optical fibre 200 μm in diameter (Thorlabs) coupled to a recording electrode (1 MΩ tungsten, A-M Systems) with an electrode/fibre tip-to-tip distance of 200–400 μm were lowered into the transduced accumbens (electrode tip 4.8–5.2 mm below bregma) of mice placed in a stereotactic frame (David Kopf Instruments) and anaesthetized under isoflurane. Light from a 473 nm diode laser (CrystaLaser) was delivered through the fibre. Electrical signals were bandpass filtered and amplified (0.3–1 kHz, 1800 Microelectrode AC Amplifier, A-M Systems) and analysed with pClamp 10.0 (Molecular Devices). Spikes were detected by threshold and individually confirmed by inspection.

Behavioural analysis. Optical stimulation was applied through an optical fibre (200 μm diameter, Thor Labs) coupled to a 473 nm blue diode laser (CrystaLaser) and registered with a cannula targeting accumbens (0–100 μm from tip). Light was delivered with 50 ms pulse width for optoXRs via a function generator (Agilent 33220A). Place preference was conducted in a standard apparatus (SD Instruments) with walls between chambers removed to permit free exploration. Data were analysed from video for amount of time spent in each chamber by two independent, blinded observers using a custom tallying script run in MATLAB (Mathworks). For open field tests, animals were placed in a square open field measuring 40 × 40 cm; light stimulation was delivered with the same parameters as for place preference experiments. Videos were analysed using automated software (Viewpoint), for total time and distance in the central 15 × 15 cm square versus the outer annulus (remainder of the field).

Statistical analysis. Where indicated, two-tailed Student's *t*-tests (calculated in Microsoft Excel) or one-way ANOVA with Tukey post-hoc tests (GraphPad Prism) were used. All summary bar graphs are presented as mean ± s.e.m., with significance denoted as follows: *$P < 0.05$, **$P < 0.01$, ***$P < 0.001$.

1. Karnik, S. S. *et al.* Activation of G-protein-coupled receptors: A common molecular mechanism. *Trends Endocrinol. Metab.* **14,** 431–437 (2003).
2. Kim, J. M. *et al.* Light-driven activation of β2-adrenergic receptor signaling by a chimeric rhodopsin containing the β2-adrenergic receptor cytoplasmic loops. *Biochemistry* **44,** 2284–2292 (2005).
3. Pierce, K. L., Premont, R. T. & Lefkowitz, R. J. Seven-transmembrane receptors. *Nature Rev. Mol. Cell Biol.* **3,** 639–650 (2002).
4. Zhang, F. *et al.* Channelrhodopsin-2 and optical control of excitable cells. *Nature Meth.* **3,** 785–792 (2006).
5. Oliveira, L., Paiva, A. C. M. & Vriend, G. A low resolution model for the interaction of G proteins with G protein-coupled receptors. *Protein Eng.* **12,** 1087–1095 (1999).
6. Palczewski, K. G protein-coupled receptor rhodopsin. *Annu. Rev. Biochem.* **75,** 743–767 (2006).
7. Azzi, M. *et al.* β-Arrestin-mediated activation of MAPK by inverse agonists reveals distinct active conformations for G protein-coupled receptors. *Proc. Natl Acad. Sci. USA* **100,** 11406–11411 (2003).
8. Kenakin, T. Special issue on allosterism and collateral efficacy. *Trends Pharmacol. Sci.* **28,** 359–446 (2007).
9. Shukla, A. K. *et al.* Distinct conformational changes in β-arrestin report biased agonism at seven-transmembrane receptors. *Proc. Natl Acad. Sci. USA* **105,** 9988–9993 (2008).

10. Rich, T. C. *et al.* In vivo assessment of local phosphodiesterase activity using tailored cyclic nucleotide-gated channels as cAMP sensors. *J. Gen. Physiol.* **118**, 63–78 (2001).
11. Wilson, C. J. in *The Synaptic Organization of the Brain* (ed. Shepherd, G.) 361–413 (Oxford Univ. Press, 2003).
12. Gradinaru, V. *et al.* Targeting and readout strategies for fast optical neural control in vitro and in vivo. *J. Neurosci.* **27**, 14231–14238 (2007).
13. Deisseroth, K. *et al.* Signaling from synapse to nucleus: The logic behind the mechanisms. *Curr. Opin. Neurobiol.* **13**, 354–365 (2003).
14. White, F. J. & Wang, R. Y. Electrophysiological evidence for the existence of both D-1 and D-2 dopamine receptors in the rat nucleus accumbens. *J. Neurosci.* **6**, 274–280 (1986).
15. Hyman, S. E., Malenka, R. C. & Nestler, E. J. Neural mechanisms of addiction: The role of reward-related learning and memory. *Annu. Rev. Neurosci.* **29**, 565–598 (2006).
16. Tobler, P. N., Fiorillo, C. D. & Schultz, W. Adaptive coding of reward value by dopamine neurons. *Science* **307**, 1642–1645 (2005).
17. Potts, J. T. & Waldrop, T. G. Discharge patterns of somatosensitive neurons in the nucleus tractus solitarius of the cat. *Neuroscience* **132**, 1123–1134 (2005).
18. Pettit, D. L. *et al.* Chemical two-photon uncaging: A novel approach to mapping glutamate receptors. *Neuron* **19**, 465–471 (1997).
19. Furuta, T. *et al.* Brominated 7-hydroxycoumarin-4-ylmethyls: Photolabile protecting groups with biologically useful cross-sections for two photon photolysis. *Proc. Natl Acad. Sci. USA* **96**, 1193–1200 (1999).
20. Conklin, B. R. *et al.* Engineering GPCR signaling pathways with RASSLs. *Nature Meth.* **5**, 673–678 (2008).
21. Lima, S. Q. & Miesenböck, G. Remote control of behavior through genetically targeted photostimulation of neurons. *Cell* **121**, 141–152 (2005).
22. Zemelman, B. V. *et al.* Selective photostimulation of genetically chARGed neurons. *Neuron* **33**, 15–22 (2002).
23. Li, X. *et al.* Fast noninvasive activation and inhibition of neural and network activity by vertebrate rhodopsin and green algae channelrhodopsin. *Proc. Natl Acad. Sci. USA* **102**, 17816–17821 (2005).
24. Schroder-Lang, S. *et al.* Fast manipulation of cellular cAMP level by light in vivo. *Nature Meth.* **4**, 39–42 (2007).
25. Cohen, G. B. *et al.* Constitutive activation of opsin: Influence of charge at position 134 and size at position 296. *Biochemistry* **32**, 6111–6115 (1993).
26. Carelli, R. M. & Wightman, R. M. Functional microcircuitry in the accumbens underlying drug addiction: Insights from real-time signaling during behavior. *Curr. Opin. Neurobiol.* **14**, 763–768 (2004).
27. Dunn, T. A. *et al.* Imaging of cAMP levels and protein kinase A activity reveals that retinal waves drive oscillations in second-messenger cascades. *J. Neurosci.* **26**, 12807–12815 (2006).
28. Zhang, F. *et al.* Multimodal fast optical interrogation of neural circuitry. *Nature* **446**, 633–639 (2007).
29. Petreanu, L. *et al.* Channelrhodopsin-2-assisted circuit mapping of long-range callosal projections. *Nature Neurosci.* **10**, 663–668 (2007).
30. Airan, R. D. *et al.* Integration of light-controlled neuronal firing and fast circuit imaging. *Curr. Opin. Neurobiol.* **17**, 587–592 (2007).